

MS-DFTVNET: A LONG-TERM TIME SERIES PREDICTION METHOD BASED ON MULTI-SCALE DEFORMABLE CONVOLUTION

Chenghan Li^{1,*} Mingchen Li^{2,*} Yipu Liao³ Ruisheng Diao^{4,†}

¹ Shenzhen International Graduate School, Tsinghua University, Shenzhen, China

² The Hong Kong University of Science and Technology (Guangzhou), Guangzhou, China

³ Department of EECS, University of Michigan, Ann Arbor, USA

⁴ ZJU-UIUC Institute, Zhejiang University, Haining, China

Email: ruishengdiao@intl.zju.edu.cn

* Equal contribution † Corresponding author

ABSTRACT

Research on long-term time series prediction has primarily relied on Transformer and MLP models, while the potential of convolutional networks in this domain remains under-explored. To address this, we propose a novel multi-scale time series reshape module that effectively captures cross-period patch interactions and variable dependencies. Building on this, we develop MS-DFTVNet, the multi-scale 3D deformable convolutional framework tailored for long-term forecasting. Moreover, to handle the inherently uneven distribution of temporal features, we introduce a context-aware dynamic deformable convolution mechanism, which further enhances the model’s ability to capture complex temporal patterns. Extensive experiments demonstrate that MS-DFTVNet not only significantly outperforms strong baselines but also achieves an average improvement of about 7.5% across six public datasets, setting new state-of-the-art results.

Index Terms— Long-Term Time Series Forecasting, CNN, Multi-Scale, Fast Fourier Transform, Deformable Convolution

1. INTRODUCTION

Long-term time series prediction is a crucial task with extremely wide applications in professional fields such as energy management [1] [2], weather forecasting [3], and health monitoring [4]. However, long-term time series forecasting tasks often involve complex multi-period scales [5] [6] and cross-variable dependencies [7], making the development of effective forecasting models a significant challenge. Time series data can be partitioned into segments of different lengths, where smaller segments provide fine-grained temporal features and larger segments capture coarse-grained temporal patterns. Local dependencies are typically reflected in short-range temporal relationships, while global dependencies arise from long-range temporal interactions [8] [9] [10](see in

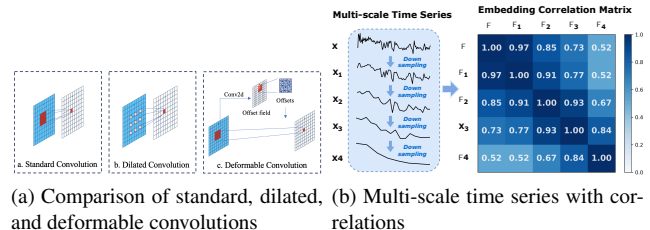


Fig. 1: Illustration of deformable convolution and multi-scale characteristics in time series data

Figure 1). Recent advances in convolutional models have demonstrated promising progress in long-term time-series forecasting. TimesNet [11], ModernTCN [12] extend convolutional approaches to capture complex temporal dynamics and global features. However, these models still fail to fully exploit the multi-scale characteristics of time series and the direct relationships across variables. Multi-scale feature modeling has proven highly effective for correlation learning and feature extraction in domains such as computer vision and multimodal learning. Yet, its potential remains underexplored in time series forecasting. Methods like Pyraformer [13], Scaleformer [14] introduce multi-scale frameworks, but often at the cost of added model complexity. Despite these advances, existing methods still face fundamental challenges in effectively modeling the intrinsic properties of time series. In particular, they struggle to adaptively capture multi-scale temporal features while simultaneously modeling direct dependencies across variables. These limitations motivate our work.

We address two major limitations in long-term time-series forecasting: (1) the lack of adaptive multi-scale feature extraction in existing models, and (2) the absence of CNN-based methods that can jointly capture multi-scale patches and cross-variable dependencies. Motivated by our prior

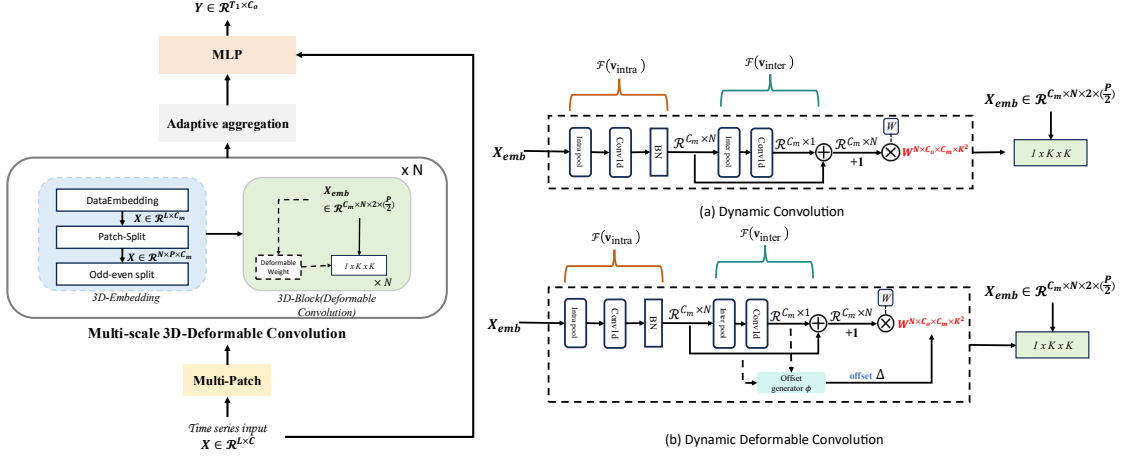


Fig. 2: Overall framework of MS-DFTVNet with the dynamic deformable convolution module.

work [7], which showed that reshaping time-series patches into 3D tensors with dynamic convolution can effectively model both time-varying and time-invariant patterns, we introduce MS-DFTVNet, an adaptive multi-scale 3D dynamic deformable convolutional network. Our key contributions are: (1) a Fourier-based adaptive patch module that enables efficient multi-scale feature extraction, and (2) a dynamic deformable convolution mechanism that captures both patch-level structures and cross-variable dependencies. Extensive evaluations on multiple public benchmarks demonstrate that MS-DFTVNet delivers consistent gains in accuracy and robustness, establishing new state-of-the-art performance.

2. PROPOSED METHOD

2.1. Problem Statement

Given a multivariate history $X_{\text{in}} \in \mathbb{R}^{L \times C}$ of length L , the goal is to forecast the future sequence $X_{\text{out}} \in \mathbb{R}^{P \times C}$ with horizon P . Let the predictor be f_{θ} , i.e., $\hat{X}_{\text{out}} = f_{\theta}(X_{\text{in}})$. The parameters θ are learned by minimizing the supervised loss $\mathcal{L}(\theta) = \frac{1}{P \cdot C} \|X_{\text{out}} - \hat{X}_{\text{out}}\|_2^2$, where mean squared error (MSE) is used by default.

2.2. Framework

The proposed method is illustrated in Figure 2. The overall architecture of MS-DFTVNet is based on a Mixer-based framework and is composed of three key modules: *Multi-Patch*, *3D Deformable Convolution*, and *Adaptive Aggregation*. Each of these modules plays a distinct role in enhancing Multi-Scale feature extraction and fusion. The *Multi-Patch* module is designed to capture local and global temporal dependencies across multiple time scales and the *3D Deformable Convolution* module dynamically adjusts its receptive field to model complex multi-scale temporal interactions more effectively.

Finally, the *Adaptive Aggregation* module integrates features from multiple paths to produce time series representations. In the following sections, we provide a detailed discussion of each component and its contribution to the model's overall performance.

Multi-Patch Module: This module utilizes the Fast Fourier transform to extract multiple dominant periods embedded within the time series adaptively. By identifying these intrinsic periodic patterns, the time series can be segmented into patches that align with the discovered periods, enabling better structural representation and improved modeling efficiency. For a time series of length L with C features, the original format is represented as $\mathcal{X}_{\text{in}} \in \mathbb{R}^{L \times C}$, where each row corresponds to a specific timestamp and each column denotes a particular variable. To effectively capture temporal dependencies across varying scales, it is crucial first to identify the underlying periodic components. This is achieved by transforming the time series into the frequency domain using the Fast Fourier Transform (FFT), which enables the detection of frequency peaks corresponding to dominant periodicities. The resulting spectral information serves as the foundation for adaptive patch segmentation, as detailed below:

$$\begin{aligned} \{f_1, \dots, f_k\} &= \arg \operatorname{Topk}_{f_* \in \{1, \dots, \lfloor \frac{T}{2} \rfloor\}} (\operatorname{Avg}(\operatorname{Amp}(\operatorname{FFT}(\mathcal{X}_{\text{in}})))) \\ p_i &= \left\lfloor \frac{T}{f_i} \right\rfloor, \quad i \in \{1, \dots, k\} \end{aligned} \quad (1)$$

where $\operatorname{FFT}(\cdot)$ and $\operatorname{Amp}(\cdot)$ represent the Fast Fourier Transform and the calculation of amplitude values, respectively. The amplitude of each frequency is computed by averaging across C dimensions using $\operatorname{Avg}(\cdot)$. This corresponds to the patch length $p_i = \frac{T}{f_i}$, where f_i denotes the frequency.

3D Deformable Convolution: We first embed the input time series along the feature dimension, mapping it from C to a high-dimensional space of C_m , resulting in the embedded representation $\mathcal{X}_{\text{in}} \in \mathbb{R}^{L \times C_m}$. This step enhances the

feature expressiveness. To segment the sequence into temporal patches(p_i), we apply a one-dimensional convolutional layer (Conv1D) with a kernel size of P , effectively dividing \mathcal{X}_{in} into $N = L/P$ patches. The output after convolution is denoted as $\mathcal{X}_{\text{emb}} \in \mathbb{R}^{N \times P \times C_m}$, where each patch preserves local temporal patterns over P time steps. Next, to further capture intra-patch structure, we split each patch into two equal-length sub-patches of size $P/2$, and then stack them along a new dimension, yielding the reshaped representation $\mathcal{X}_{\text{emb}} \in \mathbb{R}^{N \times 2 \times (P/2) \times C_m}$. This formulation enables the model to learn more nuanced dependencies within each patch. When using multiple patch lengths p_i , we can obtain a set of multi-scale embeddings $\{\mathcal{X}_{\text{emb}}^1, \dots, \mathcal{X}_{\text{emb}}^k\}$, enabling the model to capture dynamics at different temporal resolutions.

Building upon TVNet, which models dynamic amplitude modulation through $W_i = \alpha_i \cdot W_b$, we extend this formulation by additionally learning kernel *sampling shapes*. Specifically, for each scale p_i and patch n , continuous offsets $\{\Delta_{n,k}^{(i)}\}$ are generated from intra-patch and inter-patch vectors, and bounded to ensure scale-aware ranges. The output feature is then expressed as:

$$\tilde{x}_n^{(i)} = \sum_{k \in \mathcal{K}} (\alpha_{n,k}^{(i)} W_{b,k}) \cdot \Delta_{n,k}^{(i)} \quad (2)$$

where \mathcal{K} denotes kernel locations.

The weight $\alpha^{(i)}$ is generated adaptively by considering both intra-patch and inter-patch vectors, ensuring that local and global dynamics are jointly captured:

$$\alpha^{(i)} = 1 + \mathcal{F}_{\text{intra}}(\mathbf{v}_{\text{intra}}) + \mathcal{F}_{\text{inter}}(\mathbf{v}_{\text{inter}}) \quad (3)$$

where $\mathbf{v}_{\text{intra}}$ and $\mathbf{v}_{\text{inter}}$ are obtained by hierarchical pooling, followed by a lightweight Conv1D layer and ReLU activations. Beyond amplitude modulation, we further introduce shape dynamics by learning kernel sampling offsets. Specifically, offsets $\{\Delta_{n,k}^{(i)}\}$ are generated by an offset generator that reuses the same intra- and inter-patch vectors, i.e.,

$$\widehat{\Delta}_n^{(i)}(\{\widehat{\Delta}_{n,k}^{(i)}\}_{k \in \mathcal{K}}) = \Psi(\mathbf{v}_{\text{intra}}^{(i)}, \mathbf{v}_{\text{inter}}^{(i)}) \quad (4)$$

where $\Psi(\cdot, \cdot)$ denotes the offset generator. A lightweight head (e.g., 1×1 convolution with grouped linear layers) maps vectors to offsets. To stabilize training, offsets are bounded using a scaled tanh:

$$\Delta_{n,k}^{(i)} = r_t(p_i) \tanh(\widehat{\Delta}_{n,k}^{(i)}) \quad (5)$$

Empirically, we set $r_t(p_i) = \lfloor p_i/4 \rfloor$, enabling larger receptive shifts for longer periods.

Adaptive aggregation: involves fusing k distinct 3D-feature vectors $\{\mathcal{X}_{\text{emb}}^1, \dots, \mathcal{X}_{\text{emb}}^k\}$ for the subsequent layer. The amplitudes \mathcal{A} reflect the relative importance of selected frequencies and periods, corresponding to the importance of each transformed 3D tensor. We aggregate the

1D-representations based on these amplitudes:

$$\mathcal{A}_{f_1}, \dots, \mathcal{A}_{f_k} = \arg \text{Topk}(\text{Avg}(\text{Amp}(\text{FFT}(\mathcal{X}_{\text{in}})))) \quad (6a)$$

$$\hat{\mathcal{A}}_{f_1}, \dots, \hat{\mathcal{A}}_{f_k} = \text{Softmax}(\mathcal{A}_{f_1}, \dots, \mathcal{A}_{f_k}) \quad (6b)$$

$$\mathcal{X}_{\text{emb}} = \sum_{i=1}^k \hat{\mathcal{A}}_{f_i} \times \mathcal{X}_{\text{emb}}^i. \quad (6c)$$

The final prediction results are obtained using residual connections and an MLP, as shown in the following formulas:

$$Y = \text{MLP}(\mathcal{X}_{\text{emb}} + \mathcal{X}_{\text{in}}). \quad (7)$$

3. EXPERIMENT AND RESULT

In this section, we evaluate the performance of MS-DFTVNet on public datasets using Mean Squared Error (MSE) and Mean Absolute Error (MAE) as our metrics. It is worth noting that, for these metrics, a lower value indicates a superior performance. To fully validate the effectiveness of the proposed method in this paper, we conducted comparisons on six public datasets (Exchange, ETTm2, ETTh1, Electricity, Weather, ILI) with nine baselines (TVNet [7], PatchTST [15], iTransformer [16], Crossformer [17], RLIn-ear [18], MTS-Mixer [19], DLinear, TimesNet [11], and MICN [20]). Our method and baselines are optimized using the Adam optimizer. The learning rate starts at $1e^{-4}$ and is halved when loss stagnates. The loss function used is MSE. We evaluate accuracy using $MSE = \frac{1}{n} \sum_{i=1}^n (y - \hat{y})^2$ and $MAE = \frac{1}{n} \sum_{i=1}^n |y - \hat{y}|$. All models are run on a single NVIDIA 3090 GPU with 24 GB of memory.

The forecasting results are comprehensively presented in Table 1. A clear trend is observed where the prediction accuracy tends to decline progressively as the forecast horizon length increases, reflecting the inherent challenges in long-term forecasting and the accumulation of uncertainty over time. Despite this general trend, MS-DFTVNet consistently demonstrates superior performance compared to other baseline models across diverse datasets such as Exchange, ETTm2, ETTh1, Electricity, Weather, and ILI. For example, on Exchange with a horizon of 336, MS-DFTVNet achieves an MSE of 0.271 versus 0.309 for TimesNet, while on ETTm2 at 720 it records 0.343 against 0.396 for iTransformer, corresponding to relative improvements of 12–15%. Notably, the model achieves the lowest MSE and MAE in the majority of cases, highlighting its ability to capture both short-term fluctuations and long-term dependencies effectively. This advantage is particularly evident under extended forecasting horizons (e.g., 336 and 720 steps), where many Transformer-based models exhibit sharp performance degradation, while MS-DFTVNet maintains relatively stable accuracy. Such robustness suggests that the proposed multi-scale deformable convolution framework is well-suited for handling complex temporal patterns and cross-variable interactions.

Table 1: Forecasting result comparison with different horizon lengths. The lookback length is set to 24 for ILI and 96 for the others. **Red** indicates the best result, while **Blue underlining** indicates the second-best result.

Models	MS-DFTVNet		TVNet		PatchTST		iTransformer		Crossformer		RLinear		MTS-Mixer		DLinear		TimesNet		MICN		
Metrics	MSE	MAE	MSE	MAE	MSE	MAE	MSE	MAE	MSE	MAE	MSE	MAE	MSE	MAE	MSE	MAE	MSE	MAE	MSE	MAE	
Exchange	96	<u>0.081</u>	<u>0.203</u>	<u>0.080</u>	<u>0.195</u>	0.093	0.214	0.086	0.206	0.186	0.346	0.083	0.301	0.083	0.200	<u>0.081</u>	<u>0.203</u>	0.107	0.234	0.102	0.235
	192	<u>0.157</u>	<u>0.289</u>	<u>0.163</u>	<u>0.285</u>	0.192	0.312	0.177	0.299	0.467	0.522	0.170	0.293	0.174	0.296	<u>0.157</u>	0.293	0.226	0.344	0.172	0.316
	336	<u>0.271</u>	<u>0.390</u>	<u>0.291</u>	<u>0.394</u>	0.350	0.432	0.331	0.417	0.783	0.721	0.309	0.401	0.336	0.417	0.305	0.414	0.367	0.448	<u>0.272</u>	0.407
	720	<u>0.642</u>	<u>0.601</u>	0.658	<u>0.594</u>	0.911	0.716	0.847	0.691	1.367	0.943	0.817	0.680	0.900	0.715	<u>0.643</u>	0.601	0.964	0.746	0.714	0.658
ETTm2	96	<u>0.134</u>	<u>0.249</u>	<u>0.161</u>	<u>0.254</u>	0.165	0.255	0.180	0.264	0.421	0.461	0.164	0.253	0.177	0.259	0.167	0.260	0.187	0.267	0.178	0.273
	192	<u>0.201</u>	<u>0.282</u>	0.220	0.293	0.220	0.292	0.250	0.309	0.503	0.519	0.219	0.290	0.241	0.303	0.224	0.303	0.249	0.309	0.245	0.316
	336	<u>0.263</u>	<u>0.313</u>	<u>0.272</u>	<u>0.316</u>	0.274	0.329	0.311	0.348	0.611	0.580	0.273	0.326	0.297	0.338	0.281	0.342	0.312	0.351	0.295	0.350
	720	<u>0.343</u>	<u>0.366</u>	<u>0.349</u>	<u>0.379</u>	0.362	0.385	0.412	0.407	0.996	0.750	0.366	0.385	0.396	0.398	0.397	0.421	0.497	0.403	0.389	0.406
ETTh1	96	<u>0.354</u>	<u>0.392</u>	0.371	0.408	<u>0.370</u>	<u>0.399</u>	0.386	0.405	0.386	0.429	0.366	0.391	0.372	0.395	0.375	0.399	0.384	0.402	0.396	0.427
	192	<u>0.390</u>	<u>0.404</u>	<u>0.398</u>	<u>0.409</u>	0.413	0.421	0.441	0.436	0.419	0.444	0.404	0.412	0.416	0.426	0.405	0.416	0.557	0.436	0.430	0.453
	336	<u>0.399</u>	<u>0.407</u>	<u>0.401</u>	<u>0.409</u>	0.422	0.436	0.487	0.458	0.440	0.461	0.420	0.423	0.455	0.449	0.439	0.443	0.491	0.469	0.433	0.458
	720	<u>0.437</u>	<u>0.446</u>	0.458	<u>0.459</u>	<u>0.447</u>	0.466	0.503	0.491	0.519	0.524	0.442	0.456	0.475	0.472	0.472	0.490	0.521	0.500	0.474	0.508
Electricity	96	<u>0.134</u>	<u>0.221</u>	0.142	0.223	<u>0.129</u>	<u>0.222</u>	0.148	0.240	0.187	0.283	0.140	0.235	0.141	0.243	0.153	0.237	0.168	0.272	0.159	0.267
	192	0.154	<u>0.236</u>	0.165	0.241	<u>0.147</u>	<u>0.240</u>	0.162	0.253	0.258	0.330	0.154	0.248	0.163	0.261	0.152	0.249	0.184	0.289	0.168	0.279
	336	<u>0.159</u>	<u>0.260</u>	0.164	0.269	<u>0.163</u>	<u>0.259</u>	0.178	0.269	0.323	0.369	0.171	0.264	0.176	0.277	0.169	0.267	0.198	0.308	0.161	0.259
	720	<u>0.181</u>	<u>0.283</u>	<u>0.190</u>	<u>0.284</u>	0.197	0.290	0.225	0.317	0.404	0.423	0.209	0.297	0.212	0.308	0.233	0.344	0.220	0.320	0.203	0.312
Weather	96	<u>0.142</u>	<u>0.198</u>	<u>0.147</u>	<u>0.198</u>	0.149	0.198	0.174	0.214	0.153	0.217	0.175	0.225	0.156	0.206	0.152	0.237	0.172	0.220	0.161	0.226
	192	<u>0.185</u>	<u>0.237</u>	<u>0.194</u>	<u>0.238</u>	0.194	0.241	0.221	0.254	0.197	0.269	0.218	0.260	0.199	0.248	0.220	0.282	0.219	0.261	0.220	0.283
	336	<u>0.232</u>	<u>0.267</u>	<u>0.235</u>	<u>0.277</u>	0.245	0.282	0.278	0.296	0.252	0.311	0.265	0.294	0.249	0.291	0.265	0.319	0.280	0.306	0.275	0.328
	720	<u>0.302</u>	<u>0.329</u>	<u>0.308</u>	<u>0.331</u>	0.314	0.334	0.358	0.347	0.318	0.363	0.329	0.339	0.336	0.343	0.323	0.362	0.365	0.359	0.311	0.356
ILI	24	<u>1.320</u>	<u>0.703</u>	1.324	<u>0.712</u>	<u>1.319</u>	0.754	2.207	1.032	3.040	1.186	4.337	1.507	1.472	0.798	2.215	1.081	2.317	0.934	2.684	1.112
	36	<u>1.180</u>	<u>0.764</u>	<u>1.190</u>	<u>0.772</u>	1.430	0.834	1.934	0.951	3.356	1.230	4.205	1.481	1.435	0.745	1.963	0.963	1.972	0.920	2.507	1.013
	48	<u>1.395</u>	<u>0.706</u>	<u>1.456</u>	<u>0.782</u>	1.553	0.815	2.127	1.004	3.441	1.223	4.257	1.484	1.474	0.822	2.130	1.024	2.238	0.940	2.423	1.012
	60	<u>1.644</u>	<u>0.782</u>	1.652	0.796	<u>1.470</u>	<u>0.788</u>	2.298	0.998	3.608	1.302	4.278	1.487	1.839	0.912	2.368	1.096	2.027	0.928	2.653	1.085

1st Count 40 4 3 0 0 0 0 1 0 1

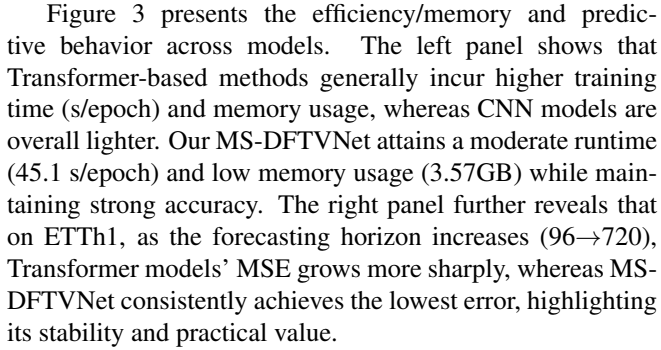


Fig. 3: Model efficiency comparison on ETTm2 with prediction length $L = 192$, and performance comparison of models with different input lengths on ETTh1 ($L = 192$).

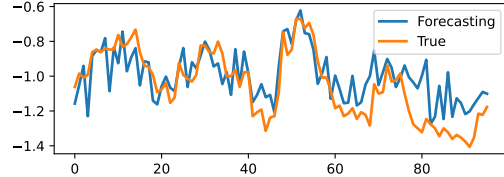


Fig. 4: Visualization of prediction results on ETTh1 with input length $L = 96$.

4. CONCLUSION

In this paper, we propose MS-DFTVNet - a multi-scale 3D deformable convolutional neural network, which demonstrates outstanding performance in long-term time series prediction. This model can efficiently capture complex temporal patterns and cross-variable dependencies, achieving high accuracy in prediction tasks. Systematic evaluations on multiple public datasets further validate its state-of-the-art performance, establishing its potential as a powerful tool for time series prediction. These results highlight the application prospects of convolutional networks in time series.

5. REFERENCES

[1] Evangelia Nivolianiti, Yannis L Karnavas, and Jean-Frederic Charpentier, “Energy management of shipboard microgrids integrating energy storage systems: A review,” *Renewable and Sustainable Energy Reviews*, vol. 189, pp. 114012, 2024.

[2] ZhaoYang Dong and Tianjing Wang, “Artificial intelligence driving perception, cognition, decision-making and deduction in energy systems: State-of-the-art and potential directions,” *Energy Internet*, vol. 1, no. 1, pp. 27–33, 2024.

[3] Ilan Price, Alvaro Sanchez-Gonzalez, Ferran Alet, Tom R Andersson, Andrew El-Kadi, Dominic Masters, Timo Ewalds, Jacklynn Stott, Shakir Mohamed, Peter Battaglia, et al., “Probabilistic weather forecasting with machine learning,” *Nature*, vol. 637, no. 8044, pp. 84–90, 2025.

[4] Aoxi Yu, Mingye Zhu, Congkai Chen, Yang Li, Haixia Cui, Shujuan Liu, and Qiang Zhao, “Implantable flexible sensors for health monitoring,” *Advanced Healthcare Materials*, vol. 13, no. 2, pp. 2302460, 2024.

[5] Siyuan Huang and Yepeng Liu, “Fl-net: A multi-scale cross-decomposition network with frequency external attention for long-term time series forecasting,” *Knowledge-Based Systems*, vol. 288, pp. 111473, 2024.

[6] Xianfang Song, Zhipeng Chen, Jun Wang, Yong Zhang, and Xiaoyan Sun, “A multi-stage lstm federated forecasting method for multi-loads under multi-time scales,” *Expert Systems with Applications*, vol. 253, pp. 124303, 2024.

[7] Chenghan Li, Mingchen Li, and Ruisheng Diao, “Tynet: A novel time series analysis method based on dynamic convolution and 3d-variation,” in *The Thirteenth International Conference on Learning Representations*, 2025.

[8] Zonglei Chen, Minbo Ma, Tianrui Li, Hongjun Wang, and Chongshou Li, “Long sequence time-series forecasting with deep learning: A survey,” *Information Fusion*, vol. 97, pp. 101819, 2023.

[9] Kun Yi, Qi Zhang, Wei Fan, Shoujin Wang, Pengyang Wang, Hui He, Ning An, Defu Lian, Longbing Cao, and Zhendong Niu, “Frequency-domain mlps are more effective learners in time series forecasting,” *Advances in Neural Information Processing Systems*, vol. 36, pp. 76656–76679, 2023.

[10] Wanlin Cai, Yuxuan Liang, Xianggen Liu, Jianshuai Feng, and Yuankai Wu, “Msgnet: Learning multi-scale inter-series correlations for multivariate time series forecasting,” in *Proceedings of the AAAI Conference on Artificial Intelligence*, 2024, vol. 38, pp. 11141–11149.

[11] Haixu Wu, Tengge Hu, Yong Liu, Hang Zhou, Jianmin Wang, and Mingsheng Long, “Timesnet: Temporal 2d-variation modeling for general time series analysis,” *arXiv preprint arXiv:2210.02186*, 2022.

[12] Donghao Luo and Xue Wang, “Moderntcn: A modern pure convolution structure for general time series analysis,” in *The twelfth international conference on learning representations*, 2024, pp. 1–43.

[13] Xiangjie Huang, Xun Lang, Tao Guo, and Li Yu, “Improving pyraformer algorithm for forecasting of 500 kv transformer bushing data with three enhanced modules,” *Electric Power Systems Research*, vol. 241, pp. 111360, 2025.

[14] Amin Shabani, Amir Abdi, Lili Meng, and Tristan Sylvestre, “Scaleformer: Iterative multi-scale refining transformers for time series forecasting,” *arXiv preprint arXiv:2206.04038*, 2022.

[15] Huiju Yi, Shengcai Zhang, Dezhi An, and Zhenyu Liu, “Patchesnet: Patchst-based multi-scale network security situation prediction,” *Knowledge-Based Systems*, vol. 299, pp. 112037, 2024.

[16] Yong Liu, Tengge Hu, Haoran Zhang, Haixu Wu, Shiyu Wang, Lintao Ma, and Mingsheng Long, “ittransformer: Inverted transformers are effective for time series forecasting,” *arXiv preprint arXiv:2310.06625*, 2023.

[17] Yunhao Zhang and Junchi Yan, “Crossformer: Transformer utilizing cross-dimension dependency for multivariate time series forecasting,” in *The eleventh international conference on learning representations*, 2023.

[18] Zhe Li, Shiyi Qi, Yiduo Li, and Zenglin Xu, “Revisiting long-term time series forecasting: An investigation on linear mapping,” *arXiv preprint arXiv:2305.10721*, 2023.

[19] Zhe Li, Zhongwen Rao, Lujia Pan, and Zenglin Xu, “Mts-mixers: Multivariate time series forecasting via factorized temporal and channel mixing,” *arXiv preprint arXiv:2302.04501*, 2023.

[20] Huiqiang Wang, Jian Peng, Feihu Huang, Jince Wang, Junhui Chen, and Yifei Xiao, “Micn: Multi-scale local and global context modeling for long-term series forecasting,” in *The eleventh international conference on learning representations*, 2023.